



A new feature extraction algorithm in face recognition

With mat lab implementation

Er. Shiva kumar

Software Engineer

Electronic and Communication Engineering

shivakumar1000@gmail.com

Empowered Security Labs Pvt Ltd

9th Block Jayanagar

Bangalore

Abstract

The face recognition is attracting much attention in the society of network multimedia information access. Areas such as network security, content indexing and retrieval, and video compression benefits from face recognition technology because "people" are the center of attention in a lot of video. Network access control via face recognition not only makes hackers virtually impossible to steal one's "password", but also increases the user-friendliness in human-computer interaction. Indexing and/or retrieving video data based on the appearances of particular persons will be useful for users such as news reporters, political scientists, and moviegoers. In this paper, the effectiveness of combining Independent Component Analysis (ICA) with Gabor algorithm (I-Gabor) as feature extraction. The features are extracted from eye and nose of known faces using Gabor and I-Gabor. The resultant features matrices were trained with support vector machine (SVM) for classification. The performances of the classification algorithms were evaluated with false acceptance rate, false rejection rate and accuracy.

Cite This Article: Er. Shiva kumar (2020). "A new feature extraction algorithm in face recognition With matlab implementation" International Journal For Development Of Computer Science And Engineering, Article Id: IJDCSE01202007, www.ijdcse.org.

Introduction

In today's networked world, the need to maintain the security of information or physical property is becoming both increasingly important and increasingly difficult. From time to time we hear about the crimes of credit card fraud, computer break-in by hackers, or security breaches in a company or government building. In the year 1998, sophisticated cyber crooks caused well over US \$100 million in losses (Reuters, 1999). In most of these crimes, the criminals were taking advantage of a fundamental flaw in the conventional access control systems: the systems do not grant access by "who we are", but by "what we have", such as ID cards, keys, and passwords, PIN numbers, or mother's maiden name. None of these means are really defining us. Rather, they merely are means to authenticate us. It goes without saying that if someone steals, duplicates, or acquires these identity means, he or she will be able to access our data or our personal property any time they want. Recently, technology became available to allow verification of "true" individual identity. [1] The aim of this research is to verify the Effectiveness of features extraction using Gabor algorithm on nose and eye in facial recognition system. Considering that we have different face images from different faces. In face detection we

are interested in highlighting those parts of the faces that are common for all faces. All the faces have eyes, lips, nose, and hair. There is need to highlight these features. The tasks that Gabor scheme can do are to remove useless and redundant data and what is left can be used for face detection.

Materials and Methods.

Features Extraction Algorithms Gabor Feature Extraction

Here the face image is processed with Gabor wavelets and in the process features are extracted. A set of frequencies and angles are chosen to represent the image at each of the above mentioned points of the wave net. Now we define “Lower bound” and “Upper bound” frequencies given by

$$fLB = 1/x_1\sqrt{2} \text{ And } fUB = 1/x_2\sqrt{2} \dots\dots\dots 1$$

The values of x_1 and x_2 are chosen such that $x_1 > x_2$. A set of frequencies to be used at each wavelet point is obtained by starting at fLB and multiplying by 2 until fUB is reached. The number of frequencies is given by P . For each frequency, a set of orientations is chosen ranging from $-\pi$ to π . The step size between any two θ is $2\pi/n$, where n is chosen appropriately. The number of orientations is given by Q . The points on the wavelet are denoted by (c_x, c_y) as per the Cartesian co-ordinates. The number of wavelet points is given by R . Now a set of frequencies “ f ” and orientations “ θ ” are obtained at each wavelet point (c_x, c_y) . Let $N = P*Q*R$ $I(x,y)$ (or just I) represents the input image. ‘ x ’ and ‘ y ’ represent the coordinates of each pixel in the Cartesian system. Hence ‘ x ’ and ‘ y ’ ranges from 0 to ‘ h ’ and ‘ w ’ respectively where ‘ h ’ is the height of the image and ‘ w ’ is the width of the image. Now we define a family of N Gabor wavelet functions $\psi = \{\psi_{1,1,1}, \dots, \psi_{P,Q,R}\}$ of the form where f_i denotes the frequency, θ_j denotes orientation and c_{xk}, c_{yk} denotes wavelet position. Now the wavelet function $\psi_{i,j,k}(x,y)$ is normalized by scaling it by the reciprocal of its length

$$\psi_{i,j,k}(x,y) = \frac{f_i^2}{2\pi} \exp\left\{-0.5f_i^2\left[(x-c_{xk})^2 + (y-c_{yk})^2\right]\right\} * \sin\left\{2\pi f_i\left[(x-c_{xk})\cos\theta_j + (y-c_{yk})\sin\theta_j\right]\right\} \dots\dots\dots 2$$

$\|\psi_{i,j,k}(x,y)\|$. Thus we obtain the unit vector $\hat{\psi}_{i,j,k}(x,y)$ as shown below. The first weight w_1 associated with wavelet ψ_1 is given by the dot product of I and $(\hat{\psi}_{i,j,k})_1$ as shown below

$$w_1 = I \cdot (\hat{\psi}_{i,j,k})_1 \dots\dots\dots 3$$

The subsequent weights w_u ($2 \leq u \leq N$) associated with wavelets ψ_u are given by the dot products of

$$(\hat{\psi}_{i,j,k})_u$$

and as shown below

$$W_u = I_{diff_u} \cdot (\hat{\psi}_{i,j,k})_u \dots\dots\dots 4$$

Where I_{diff_u} represents the intermediate difference image given by

$$I_{diff_u} = I_{diff_{(u-1)}} - \hat{I}_{u-1} \text{ with } I_{diff_1} = I(x,y), \text{ for } 2 \leq u \leq N \dots\dots\dots 5$$

Where \hat{I}_{u-1} is the intermediate reconstructed image for each wavelet given by

$$\hat{I}_u = W_u \cdot (\hat{\psi}_{i,j,k})_u, \text{ for } 1 \leq u \leq N \dots\dots\dots 6$$

The final reconstructed image is given by

$$\hat{I} = \sum_{u=0}^{N-1} \hat{I}_u \dots\dots\dots 7$$

In the above reconstruction process, the set of weights are obtained. From this set of weights the ‘n’ highest weights are selected, where ‘n’ is chosen suitably. These ‘n’ weights along with their corresponding set of ‘n’ frequencies and orientations are the features. Thus we now obtain a “n*3” feature vector. (Other methods can also be used to choose the feature vectors such as, considering only the maximum projections, considering the frequency and orientation at each point that gives maximum projection, etc). This feature vector is fed to the neural network for training or recognition as the case maybe.

Independent Gabor (I-Gabor)

Independent Gabor Features (I-Gabor) method applies the independent component analysis on the (lower dimensional) Gabor feature vector defined by $y^{(p)} = P^i X^{(p)}$. In particular, the Gabor feature vector $X^{(p)}$ of an image is first calculated. PCA then reduces the dimensionality of the Gabor feature vector and derives the lower dimensional feature vector. Finally, the I-Gabor method derives the overall (the combination of the whitening, rotation, and normalization transformations) ICA transformation matrix, F, as defined by $\Sigma y = F F^t$. The new feature vector, $Z^{(p)}$, of the image is thus defined as follows:

$$Y^{(p)} = F Z^{(p)} \dots\dots\dots 8$$

The next step after the extraction of an appropriate set of features is the classifier design. When the underlying probability density functions are known, the Bayes classifier yields the minimum error. This error, called the Bayes error, is the optimal measure for feature effectiveness when

classification is of concern, since it is a measure of class separability. proposed the Probabilistic Reasoning Model (PRM) method which defines a Bayes linear classifier under the assumption that the within class covariance matrices are identical and diagonal. Such an assumption is especially reasonable for the I-Gabor method, since the features derived by the I-Gabor method have independent components (note that the ‘identical and diagonal’ assumption takes place after the ICA transformation rather than before it). As a result, the IGF method applies the MAP Bayes rule via the PRM method for classification. In particular, Let M_k^0 ; $k = 1, 2, \dots, L$, be the mean of the training samples for class w_k after the ICA transformation. The I-Gabor method exploits, then, the following MAP classification rule of the PRM method;

$$\sum_{i=1}^m \frac{(z_i - m_{ki})^2}{\sigma_i^2} = \min_j \left\{ \sum_{i=1}^m \frac{(z_i - m_{ji})^2}{\sigma_i^2} \right\} \rightarrow Z^{(p)} \in \omega_k \dots\dots\dots 9$$

Where z_i and $m_{ki} = 1, \dots, m$, are the

components of $Z^{(p)}$ and M_k^0 respectively, and σ_i^2 is estimated by sample variance in the one dimensional ICA space:

$$\sigma_i^2 = \frac{1}{L} \sum_{k=1}^L \left\{ \frac{1}{N_k - 1} \sum_{j=1}^{N_k} (y_{ji}^{(k)} - m_{ki})^2 \right\} \dots\dots\dots 10$$

Where $y_{ji}^{(k)}$ and is the i -th element of the ICA feature $Y_j^{(k)}$ of the training image that belongs to class w_k and N_k is the number of training images available for class. The MAP classification rule of Eq. 9 thus classifies the image feature vector, $Z^{(p)}$, as belonging to the class w_k .

Methodology

Image Acquisition and Analysis Section

The input to this section is the facial image of the person seeking recognition. The image is preprocessed if required. This preprocessing involves the use of digital image enhancement techniques. Here we are assuming only variations with respect to the quality of the image and not with respect to the head poise or expressions. After the preprocessing step has been completed we need to convert the image to the portable gray map format (PGM format). This makes the image a gray scale image. Once the image has been fed to the program, we have to place the wavelets in the “Region of Importance”. As our images are faces the region of importance is “The inner face region”. Four points are located on the inner face region as shown in figure 1. The red dots indicate the corners of the eyes (represented by points 1 and 2 for outer and 3, and 4 for inner), corners of nose (represented by points 5 and 6)

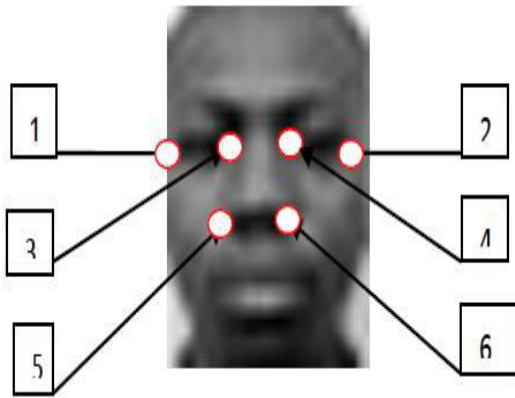
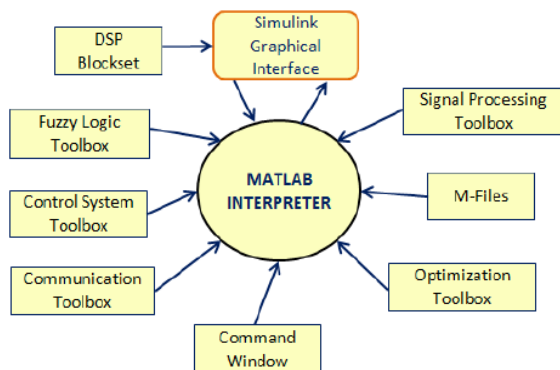


Figure 1: Indicates the initial points that are to be placed in order to create the wavenet. The distances between points 1 and 3; 1 and 5; 3 and 5; 2 and 6; 4 and 6; and 2 and 4; are calculated. Now the wavelet net (wavelet) is created and placed in the inner region of the face. The system is more efficient if these feature points are made to be located automatically rather than manually. More wavelet points gives better representation but at the cost of computational speed. Finding an appropriate tradeoff between these two factors is of prime importance.

Introduction To The Software Used

Overview of the Matlab Environment The name MATLAB stands for matrix laboratory, originally written to provide easy access to matrix software developed by the LINPACK and EISPACK projects. Today, MATLAB engines incorporate the LAPACK and BLAS libraries, embedding the state of the art in software for matrix computation. MATLAB is an interactive, matrix based system for scientific and engineering numeric computation and visualization. Its basic data element is an array that does not require dimensioning. It is used to solve many technical computing problems, especially those with matrix and vector formulation, in a fraction of the time it would take to write a program in a scalar non interactive language such as C or FORTRON



Experimental Dataset

Publicly available AT&T database is used for recognition experiments. In the database, 10 different images of each of 40 persons (total 400 images) with variations in face angles, facial expressions and facial details are considered.



RESULTS

Computational Efficiency of the SOM Method is as shown in Table 1 and Fig.

Training

In preparing the data, 300 images containing faces (eye and nose), that is, 10 different images for each of the 30 distinct subjects were used. We assume that unknown faces will yield the same results. For some subjects, the images were taken at different times, varying the lighting, facial expressions (open/closed eyes, smiling/not smiling) and facial details (glasses/no glasses). Examples of eye and nose training images are shown in Fig. (1). All the images were taken against a dark homogeneous background with the subjects in an upright, frontal position (with tolerance for some side movement).

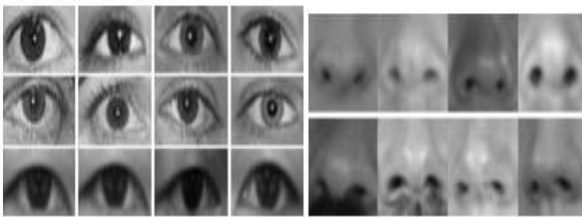


Fig. 1: Facial Features training images

The coloured images in the database were read and converted into gray-scale image with pixel values between 0(black) and 255(white). The gray-level value of the pixels were changed by multiplying the pixel value with Contrast (C) and adding it with the Brightness (B) in a linear way. This means that the same image with the same face is either dark or bright. Each face in the training set is transformed into the face space and its components are stored in memory. The

face space has to be populated with these known faces. An input face is given to the system, and then it is projected onto the face space. The number of basis vectors for each subspace is optimized experimentally. Hence, 20 vectors are found sufficient for eye subspace, while 30 vectors are sufficient for nose subspace. The resultant vectors are training using support vector machine of MATLAB 7.0.

Results

This section presents the comparative analysis of the proposed approach. Our database is composed of 300 images with 10 different images for each of the 30 distinct subjects. 150 images used for training and 150 for testing for known faces. The results are compared using the recognition accuracy of the approaches. Computing the false acceptance rate (FAR) and false rejection rate (FRR) is the common way to measure the biometric recognition accuracy. FAR is the percentage of incorrect acceptances i.e., percentage of distance measures of different people's images that fall below the threshold. FRR is the percentage of incorrect rejections i.e., percentage of distance measures of same people's images that exceed the threshold. The following table gives the percentage of the recognition rates and the accuracy rates.

Table 1: Performance of Gabor and I-Gabor on our database.

Facial parts extracted by Gabor/I-Gabor	SVM		
	FAR (%)	FRR (%)	Accuracy (%)
Face recognition based on Eye by Gabor	4.4	5.3	87.7
Face recognition based on Eye by I-Gabor	2.8	3.9	94.9

In this table, we estimate the measures for on both eye and nose using Gabor and I-Gabor for features extraction and SVM for recognition. Here we observe that I-Gabor gives a lower value in both FAR and FRR error rates on both facial parts. At the same time, the I-Gabor has a higher recognition accuracy compared to only Gabor.

Conclusion

Face recognition is a both challenging and important recognition Technique, The face detection system is created with Gabor feature extraction and. In this paper, an automatic method to detect eye and nose location from facial images based on the response of face regions to feature subspaces is presented. These feature points are obtained from the special characteristics of each individual face, which are compared in terms of nose and eyes. In order to further

improve the performance of the method, we employed SVM for further classifications on local characteristics of facial features regions. The results are quite encouraging but there is still need for further studies to improve system. We hope this paper can provide the readers a better understanding about face recognition, and we encourage the readers who are interested in this topic to go to the references for more detailed study.

References

An Introduction to Face Recognition Technology Shang-Hung Lin. Informing science special issue on multimedia informing technologies, part 2 volume3no1,2000.

Ingvar, A. (1994). Dielectric and conductivity studies of polymer electrolytes. Chalmers University of Technology and University of Gothenburg.

Kumar, D., & Hashmi, S.A. (2010). Ionic liquid based sodium ion conducting gel polymer electrolytes, Solid State Ionics, 181(1), 416-423.

Pan, H., Hu, YS. & Chen L. (2013) Room-temperature stationary sodiumion batteries for large-scale electric energy storage. Energy & Environ Sci., 6:2338e60.